Science of the Total Environment 642 (2018) 638–645

Contents lists available at ScienceDirect

Science of the Total Environment

journal homepage: www.elsevier.com/locate/scitotenv

Particle-scale understanding of cypermethrin in sediment: Desorption, bioavailability, and bioaccumulation in benthic invertebrate *Lumbriculus variegatus*

Jie Zhang [a], Jing You [a], Huizhen Li [a,*], W. Tyler Mehler [a,b], Eddy Y. Zeng [a]

[a] School of Environment and Guangdong Key Laboratory of Environmental Pollution and Health, Jinan University, Guangzhou 510632, China
[b] School of Biosciences, Centre for Aquatic Pollution Identification and Management, The University of Melbourne, Parkville, Victoria 3010, Australia

HIGHLIGHTS

- Impact of particle size on bioaccumulation potential of cypermethrin was evaluated.
- Desorption of cypermethrin in sediment increased with decreasing grain size.
- Chemical activity of cypermethrin in fine sediment was lower than coarse sediment.
- Particle size showed no impact on the BSAFs of cypermethrin in the benthic worms.

GRAPHICAL ABSTRACT

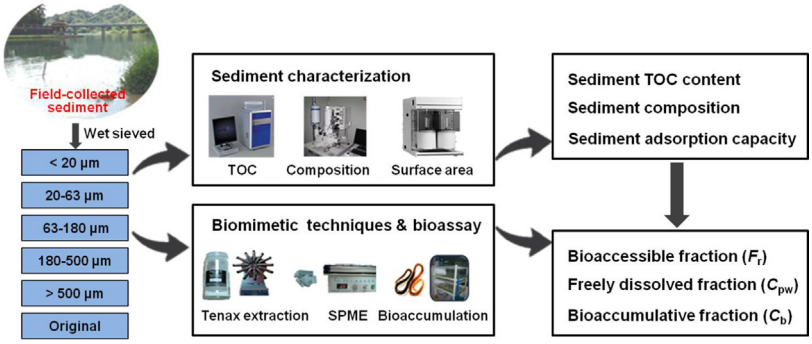

ARTICLE INFO

Article history:
Received 12 April 2018
Received in revised form 4 June 2018
Accepted 8 June 2018
Available online xxxx

Editor: Jay Gan

Keywords:
Sediment particle size
Consecutive Tenax extraction
Solid-phase microextraction
Bioaccumulation
Benthic invertebrates
Cypermethrin

ABSTRACT

Influence of sediment particle size on the desorption, bioavailability, and bioaccumulation potential of cypermethrin was investigated in the present study using two biomimetic techniques (Tenax extraction and solid-phase microextraction (SPME)) and bioaccumulation testing with *Lumbriculus variegatus*. A field-collected sediment was wet sieved to obtain five particle-size fractions (<20, 20–63, 63–180, 180–500, and >500 μm) and used for cypermethrin spiking. The finest sediment (<20 μm) had the highest rapid desorption fraction (F_r) and rate (k_r) when compared to coarser sediments. Elimination rate constants of cypermethrin determined by SPME ($k_{e\text{-SPME}}$) and *L. variegatus* ($k_{e\text{-}L.v.}$) for various fractions of sediments followed the same trend, suggesting SPME fiber acts as a good surrogate for benthic organisms considering passive partitioning. Finally, biota-sediment accumulation factors (BSAFs) of cypermethrin in worms were almost the same among the sediments with different particle sizes (0.425 ± 0.07–0.445 ± 0.07 g OC g^{-1} lipid), suggesting that the differences in desorption and freely dissolved concentrations of cypermethrin did not significantly influence its bioaccumulation potential in worms. Selective ingestion of fine sediment particles may be one of the contributing reasons for no differences in BSAFs observed in the treatments as would have been expected. The different desorption and freely dissolved concentrations of cypermethrin in sediments with different particle sizes observed in this study highlights the need for further work to better understand the influence of particle size on the toxicity of highly toxic insecticides, such as cypermethrin, to sensitive benthic species.

* Corresponding author.
E-mail address: lihuizhen@jnu.edu.cn (H. Li).

https://doi.org/10.1016/j.scitotenv.2018.06.098
0048-9697/

1. Introduction

Increasing water insecticide contamination and associated decreasing regional aquatic biodiversity are evident worldwide (Stehle and Schulz, 2015a). Newer-generation insecticides (e.g., pyrethroids) had higher exceedances of regulatory thresholds than legacy ones (e.g., organochlorine pesticides) (Stehle and Schulz, 2015a; Stehle and Schulz, 2015b). Thus, it is of great importance to assess and control potential risk caused by newer-generation insecticides in aquatic systems. As hydrophobic insecticides tend to be bound to suspended particles and accumulated in sediment (Katagi, 2006), they pose great risk to benthic organisms (Stehle and Schulz, 2015b).

Sediments are heterogeneous at various aggregate and particle scales (Luthy et al., 1997). The transport behavior of insecticide-binding particles in flowing water system is particle-size selective, i.e., coarse particles tend to be transported by bottom currents and settle faster than fine particles. In addition, fine particles are potentially more to be resuspended to the upper water column and transported to distant areas than coarse particles (Eisma, 1993; Gan et al., 2005). The different transport mechanisms of these particles can result in location-dependent distribution of size fractionated sediments as well as differing insecticide residues, especially as fine particles normally contain larger amounts of organic matter than coarse particles (Ghosh et al., 2000; Kukkonen and Landrum, 1996; Richards et al., 2016).

Particle size takes into account of the impacts of not only organic carbon (OC) content, but also OC type, composition, surface and micropore adsorption capacity, as all of these characteristics are particle-size dependent (Jia and Gan, 2014; Wang and Keller, 2008; Zhang et al., 2016). Fine sediment particles have been reported to exhibit stronger sorption capacity for hydrophobic compounds than coarse particles, likely because surface area and organic carbon content increase with decreasing particle size (Qi et al., 2014). Enrichment of chemicals in fine sediment particles and selective ingestion of fine particles by benthic organisms are critical factors that potentially influence the bioavailability and toxicity of chemicals in sediment (Xia et al., 2016). Therefore, it is of great importance to study the influence of particle size on the desorption and bioavailability of sediment-associated hydrophobic organic compounds (HOCs), particularly those with high toxicity to benthic organisms, such as pyrethroids.

Sediment contamination of pyrethroids has been widely reported in urban and agricultural areas, and their major contribution to the high lethality of sediments to benthic invertebrates has gained public attention (Kuivila et al., 2012; Li et al., 2017; Mehler et al., 2011; Weston et al., 2004). High intrinsic toxicity of pyrethroids to non-target organisms is an important reason for their major contribution to sediment toxicity. For example, the median lethal concentrations (LC50) of cypermethrin to *Hyalella azteca* and *Chironomus dilutus* were reported at 0.38 and 1.34 μg g^{-1} OC, respectively, in 10–d sediment bioassays (Maund et al., 2002). Due to high intrinsic toxicity of pyrethroids, subtle uncertainty in sediment concentration quantification caused by particle-size distribution may lead to over- or under-estimation of toxicity (You et al., 2008).

The main objective of the present study was to evaluate the influence of particle size on the desorption, bioavailability, and bioaccumulation potential of cypermethrin in benthic invertebrates, which were quantified by consecutive Tenax extraction, solid-phase microextraction (SPME), and bioaccumulation testing using *Lumbriculus variegatus*, respectively.

2. Materials and methods

2.1. Sediment collection, sieving, and spiking

A sediment sample collected from a drinking water reservoir in Conghua, Guangdong Province, China was chosen as the original sediment to prepare different size-fractionated sediments by wet sieving. Previous toxicity testing showed that the sediment exhibited no chronic toxicity to benthic invertebrates, including *L. variegatus*, *H. azteca*, and *C. dilutus* (Du et al., 2013; Zhang et al., 2013). Additionally, cypermethrin was not detected in the sediment. Surface sediment (the top 5 cm) was collected using a stainless steel grab sampler and sieved through a 2–mm sieve to remove large debris and rocks onsite, transported back to the laboratory, and stored at 4 °C prior to use. The field-collected sediment (referred to the "original sediment" thereafter) was wet sieved to obtain five particle-size fractions, i.e., <20, 20–63, 63–180, 180–500, and >500 μm, with moisture contents ranging from 46% to 65%. The total organic carbon (TOC) content of each sediment fraction was measured with an Elementar (Vario EL III, Hanau, Germany) after removal of inorganic carbon with 1 mol L^{-1} HCl. The composition and texture of each sediment fraction were also characterized using a scanning electron microscope (SEM SU8010, Hitachi, Japan) with an accelerating voltage of 1.5 kV. Meanwhile, the surface area, pore volume, and adsorption capacity of the sediments were determined with a surface area and porosity analyzer (ASAP 2460, Micromeritics, USA) upon exposure to liquid nitrogen at −196 °C for 12 h.

Cypermethrin was spiked individually into the six sediments (original and five fractions of sediment) at nominal concentrations ranging from 31.1 to 34.8 ng g^{-1} dry wt. (Table S1), using acetone as the carrier (33 μL acetone kg^{-1} sediment maximum). Preliminary testing showed no adverse effects to *L. variegatus* when exposed to sediment containing cypermethrin at this concentration. Spiked sediments were thoroughly mixed using a stainless paddle driven by an overhead motor for 2 h, and aged at 4 °C in dark for 30 d. All sediments were re-homogenized before testing.

2.2. Biomimetic extraction

Consecutive Tenax extraction technique was used to measure the desorption rates of cypermethrin in the various sediment size fractions. Tenax extraction was performed in triplicate with six sampling time points (3, 6, 24, 72, 168, and 336 h). Five grams of each wet sediment, 50 μL of 0.1 g L^{-1} NaN_3, 45 mL of reconstituted water, 2 pieces of copper sheets, and 0.5 g Tenax beads (60–80 mesh, Scientific instrument services, NJ, USA) were added to a 50-mL screw-cap glass tube. The tube was rotated at 20 rpm on a tube rotator (QB-228, Kylin-Bell, China) at 23 °C. At each time point, Tenax beads were removed from sediment slurry, and fresh Tenax beads were added to continue the testing.

Disposable SPME fibers with a diameter core of 1000 μm and 30-μm coating of polydimethylsiloxane (Fiberguide industries, NJ, USA), were used to measure the freely dissolved concentrations of cypermethrin in sediment porewater. A stainless envelope with 10 pieces of 1-cm SPME fibers, 10 g of wet sediment, 10 mL of reconstituted water, 50 μL of 0.1 g L^{-1} of NaN_3, and 2 pieces of copper sheets were added to a 20-mL glass vial. The vial was horizontally shaken on a shaker (HY-4A, Aohua Company, China) at 120 rpm. The testing was conducted in triplicate. At each time point (24, 48, 96, 168, 336, and 672 h), an envelope with SPME fibers was withdrawn from sediment. The detailed pretreatment, extraction and cleanup processes of Tenax beads and SPME fibers are described in the Supplementary Data.

2.3. Bioaccumulation testing

Bioaccumulation testing was conducted using the oligochaete, *L. variegatus*, in accordance with the United States Environmental Protection Agency protocols (USEPA, 2000). Due to the limited amount of 20–63 and >500 μm sediments, bioaccumulation testing was only conducted with the original sediment and three size sediment fractions (<20, 63–180, and 180–500 μm). The bioaccumulation testing was performed in triplicate using 400-mL beakers containing 80 g of wet sediment, 200 mL of reconstituted water, and 20 worms. Sediment and reconstituted water were added to each beaker and allowed to settle overnight before adding test organisms. The bioassay was conducted under a light:dark photoperiod of 16:8 h, and overlying water was

renewed twice a day using an automated water-delivery system (Mehler et al., 2018). Water parameters, including dissolved oxygen, temperature, conductivity, and pH, were monitored daily, while ammonia was measured at the beginning and the end of the bioaccumulation testing. No feeding was performed during the tests. At each time point (24, 48, 96, 168, and 336 h), worms were sieved from the sediment with a 500-μm sieve and transferred to clean reconstituted water for gut purging for 6 h. The worms were then blotted dry with tissue paper and weighed using a microbalance (Sartorius Ag Pro 11, Gottingen, Germany). One worm from each replicate was used for lipid analysis and the remaining worms were used for body residue analysis. All collected organisms were stored at −20 °C prior to analysis.

2.4. Sample extraction and instrumental analysis

Cypermethrin in sediment was extracted using accelerated solvent extraction (ASE), Soxhlet extraction, and ultrasound-assisted microextraction (UAME) for confirmation purpose. The extracts were then purified using a solid phase extraction cartridge containing 600 mg of primary secondary amine, 300 mg of graphite carbon black, and 50 mg of anhydrous Na_2SO_4. Cypermethrin in worms was extracted by acetone using a tissue homogenizer (TissuePrep TP-24, Bio-xplorer Company, China). The supernatant was decanted and 1 mL of fresh acetone was added to initiate the extraction for additional two cycles. The extracts were combined and centrifuged, and the supernatant was decanted, concentrated, and solvent exchanged to hexane. The extracts were purified using 50% H_2SO_4 for three circles and finally filtered using an anhydrous Na_2SO_4 cartridge to remove residual water. Cypermethrin and the surrogate decachlorobiphenyl in Tenax, SPME, sediment, and worms were measured with a Shimadzu QP 2010 Plus series GC–MS (Shimadzu, Kyoto, Japan) in negative chemical ionization (NCI) mode after adding internal standards. Detailed descriptions of the extraction, cleanup, and instrumental analysis are presented in the Supplementary Data.

2.5. Quality assurance and quality control (QA/QC)

A batch of QA/QC samples, including a laboratory solvent blank, matrix blank, matrix spike, and matrix spike duplicate, were analyzed every 20 samples. In addition, a calibration standard was analyzed for every 20 samples to ensure the variation of calibration for each analyte was within 20%. The recoveries of cypermethrin in matrix spikes for Tenax beads, sediment samples determined by ASE, Soxhlet extraction, and UAME, and worms were 98 ± 7%, 112 ± 10%, and 98 ± 11%, respectively. The recovery of the surrogate decachlorobiphenyl in all samples was 95 ± 15%.

2.6. Data analysis

Statistical comparison was performed using a student's *t*-test ($\alpha = 0.05$). The kinetic rates and cypermethrin concentrations in *L. variegatus* at steady state and on SPME fiber at equilibrium were modeled using Scientist 2.01 (MicroMath Scientific, St. Louis, MO, USA). The desorption rates of cypermethrin measured by consecutive Tenax extractions were simulated with a biphasic desorption model (Eqs. (1) and (2)):

$$\frac{S_t}{S_0} = F_r\left(e^{-k_r t}\right) + F_s\left(e^{-k_s t}\right) \quad (1)$$

$$F_r + F_s = 1 \quad (2)$$

where S_t and S_0 are the amounts of cypermethrin in sediment (ng) at time t (h) and zero, respectively; F_r and F_s are the rapid and slow desorption fractions, respectively, and k_r and k_s are their respective rapid and slow desorption rates (h^{-1}). The rapid desorption concentration of cypermethrin in sediment ($C_{s\text{-}rap}$), which was considered as bioaccessible concentration, was calculated by Eq. (3):

$$C_{s\text{-}rap} = F_r \times C_0 \quad (3)$$

where C_0 is sediment concentration at time zero (μg g^{-1} OC).

The elimination rate constants (k_e, h^{-1}) and concentrations of cypermethrin on SPME fibers at equilibrium and *L. variegatus* at steady state were modeled with a first-order one-compartment model (Eq. (4)). The concentration of cypermethrin in sediment porewater (C_{pw}) was calculated using Eq. (5):

$$C_t = C\left(1 - e^{-k_e t}\right) \quad (4)$$

$$C_{pw} = \frac{C_f}{K_{fw}} \quad (5)$$

where C_t and C represent the concentrations of cypermethrin on the fiber or worm at time t (h) and at equilibrium (for SPME fibers) or at steady state (for worms), respectively. The C_f is the equilibrium concentrations on fiber. The log K_{fw} is PDMS-water partitioning coefficient and a value of 5.99 ± 0.12 is used for calculation (Lao et al., 2012).

Bioaccumulation potential of sediment-bound cypermethrin in *L. variegatus* was described using biota-sediment accumulation factor (BSAF), which is calculated by dividing lipid-normalized biota concentration (C_b) by OC-normalized sediment concentration (C_s).

$$\mathrm{BSAF} = \frac{C_b}{C_s} \quad (6)$$

3. Results and discussion

3.1. Sediment characterization

The field-collected sediment was wet sieved resulting in five size fractions, i.e., <20, 20–63, 63–180, 180–500, and >500 μm, and these size fractions accounted for 81.3%, 0.93%, 14.6%, 2.86%, and 0.31% of the original sediment, respectively. The SEM images confirmed the size of each sediment fraction and provided additional information regarding the composition and texture of the sediments (Fig. 1A). As expected, adsorption/desorption surface area, pore volume, and sorption capacity of the sediments increased with decreasing particle size (Fig. 1B). The results supported the notion that fine sediment particles had higher likelihood to reduce bioavailability of bound chemicals due to higher binding capability than coarse sediment particles (Ghosh et al., 2000). Based on SEM images and sediment property analysis, these five fractions were grouped into four different sediment textures or compositions, i.e., clay (<20 μm), silt (20–63 and 63–180 μm), sand (180–500 μm), and biological material (>500 μm) (Peng et al., 2014).

The TOC contents of the original and five fractionated sediments (<20, 20–63, 63–180, 180–500, and >500 μm) were 1.83 ± 0.14%, 1.78 ± 0.02%, 0.82 ± 0.12%, 1.04 ± 0.12%, 1.66 ± 0.15%, and 7.99 ± 1.80%, respectively (Table 1). The TOC content of <20 μm sediment was significantly higher than those of 20–63 and 63–180 μm sediments, which was consistent with previous observation that organic carbon enriches in fine sediments (Gan et al., 2005). Surprisingly, the sediment with the largest particle size (>500 μm) contained four times higher TOC than the other size fractions. Previous studies have shown that different TOC contents occurred in sediment particles with various composition and adsorption capacity (Di Toro et al., 1991; Ghosh et al., 2003). The >500 μm sediment has been reported to consist of a large proportion of biological materials which has high OC (Turner et al., 2017), thus it was reasonable that the TOC in this size fraction was much higher than the other size fractions. The TOC content in the 180–500 μm sediment was comparable to that in sediments at smaller sizes (i.e., <20 μm), probably due to existence of some biological materials in this

(A)

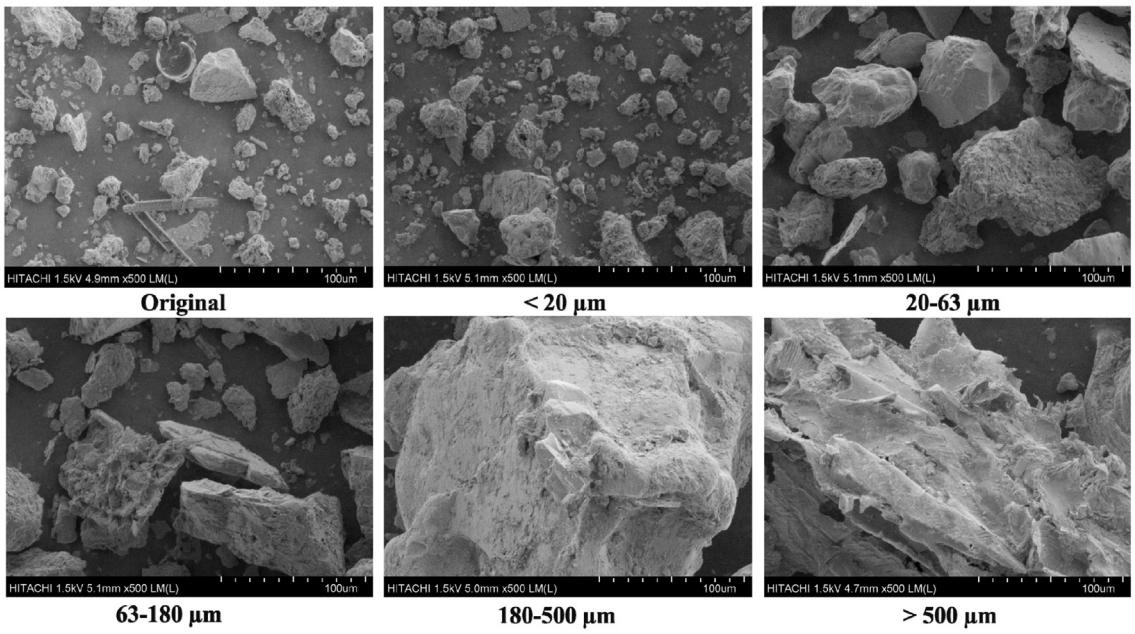

(B)

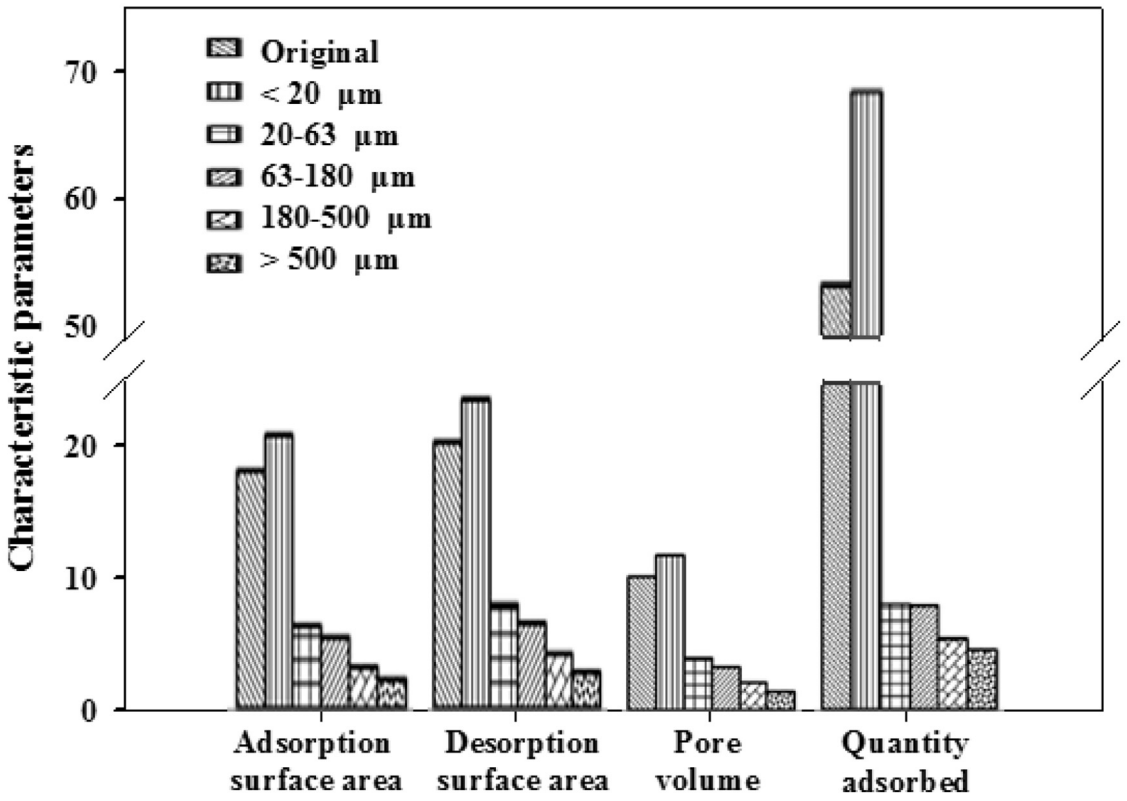

Fig. 1. (A) Visual images of the original and five fractionated sediments taken with a scanning electron microscope (SEM). (B) The adsorption surface area ($m^2\ g^{-1}$), desorption surface area ($m^2\ g^{-1}$), pore volume ($10^{-2}\ cm^3\ g^{-1}$), and quantity adsorbed ($cm^3\ g^{-1}$ STP) of the original and five fractionated sediments.

sediment, although this size fraction as a whole was observed to be dominated by sand particles. As such, both particle size and texture influenced TOC contents in sediment, which further influenced bioaccessibility/bioavailability of organic contaminants in sediment (Ghosh et al., 2003).

Table 1
The modeled parameters of cypermethrin in the original and fractionated sediments (<20, 20–63, 63–180, 180–500, and >500 μm).

Parameters	Original	<20 μm	20–63 μm	63–180 μm	180–500 μm	>500 μm
TOC (%)	1.83 ± 0.14^{a}	1.78 ± 0.02^{a}	0.817 ± 0.12^{b}	1.04 ± 0.12^{b}	1.66 ± 0.15^{a}	7.99 ± 1.8^{c}
F_r	0.391 ± 0.10^{acde}	0.689 ± 0.031^{b}	0.470 ± 0.035^{c}	0.552 ± 0.030^{d}	0.393 ± 0.023^{e}	0.259 ± 0.043^{a}
F_s	0.607 ± 0.10^{ace}	0.300 ± 0.024^{b}	0.526 ± 0.035^{c}	0.432 ± 0.028^{d}	0.601 ± 0.021^{e}	0.728 ± 0.035^{a}
k_r	0.269 ± 0.091^{a}	0.187 ± 0.018^{a}	0.122 ± 0.016^{b}	0.110 ± 0.014^{b}	0.175 ± 0.019^{a}	0.133 ± 0.053^{ab}
k_s (10^{-2})	3.37 ± 0.64^{a}	0.367 ± 0.071^{b}	1.05 ± 0.10^{c}	0.381 ± 0.051^{b}	0.909 ± 0.054^{c}	0.230 ± 0.032^{d}
C_{pw}	12.3 ± 0.079^{a}	9.48 ± 0.95^{b}	31.7 ± 0.91^{c}	18.8 ± 2.3^{d}	12.3 ± 0.55^{a}	7.25 ± 0.38^{e}
$k_{e\text{-SPME}}$ (10^{-2})	4.98 ± 0.13^{a}	1.80 ± 0.51^{b}	4.34 ± 0.49^{ac}	1.14 ± 0.41^{b}	3.14 ± 0.60^{c}	4.24 ± 0.93^{ac}
$k_{e\text{-}L.v.}$ (10^{-2})	4.80 ± 0.62^{a}	2.33 ± 0.68^{b}	-	5.93 ± 2.4^{abc}	6.25 ± 1.5^{c}	-
BSAF	0.608 ± 0.04^{a}	0.445 ± 0.07^{b}	-	0.425 ± 0.07^{b}	0.426 ± 0.05^{b}	-

The modeled parameters include: the rapid and slow desorption fractions (F_r and F_s) and their corresponding rapid and slow desorption rate constants (k_r and k_s, h^{-1}) determined using Tenax extraction ($n = 3$); the freely dissolved concentration in porewater (C_{pw}, pg L^{-1}) and the elimination rate constant ($k_{e\text{-SPME}}$, h^{-1}) determined using solid phase microextraction (SPME, $n = 3$); the elimination rate constant ($k_{e\text{-}L.v.}$, h^{-1}) via sediment bioaccumulation bioassays with *Lumbriculus variegatus* ($n = 3$) and biota-sediment accumulation factor (BSAF, g OC g^{-1} lipid); Data are presented as the mean ± standard deviation; Different superscript letters indicate significant differences among the size fraction treatments; The hypen (-) indicates that this treatment was not evaluated for this given parameter.

3.2. Desorption and bioavailability of sediment-associated cypermethrin

Biomimetic parameters, including rapid and slow fractions (F_r and F_s) and their respective kinetic rates (k_r and k_s) determined by consecutive Tenax extraction as well as elimination rate constants ($k_{e\text{-SPME}}$) and freely dissolved concentration in porewater (C_{pw}) determined by SPME, for each size fraction of sediment are shown in Table 1. Furthermore, desorption and uptake curves of cypermethrin in various sediment size fractions determined by consecutive Tenax extractions and SPME are presented in Fig. 2 and Fig. S1, respectively. The calculations were all based on sediment concentrations measured with ASE.

The desorption curve of the original sediment unexpectedly fell below zero (Fig. 2), suggesting that Tenax extractable concentration was higher than the supposed exhaustive concentration of cypermethrin in sediment measured by ASE. A similar phenomenon was observed in a previous study which showed that 45% of the evaluated desorption curves for pyrethroids were negative (Nutile et al., 2017). To evaluate the effectiveness of the extraction method, two additional exhaustive extraction methods, namely Soxhlet extraction and UAME, were used to determine the exhaustive concentrations of cypermethrin in the sediments. Sediment concentrations of cypermethrin determined by ASE, Soxhlet extraction, and UAME accounted for 65 ± 6.4%, 54 ± 14%, and 41 ± 8.5%, respectively, of the nominal concentrations after 30-d aging (Table S1), suggesting ASE was the most effective among the three methods. Desorption parameters modeled using sediment concentrations determined by ASE were all positive (Table 1). Therefore, sediment concentrations determined by ASE were applied in further analysis.

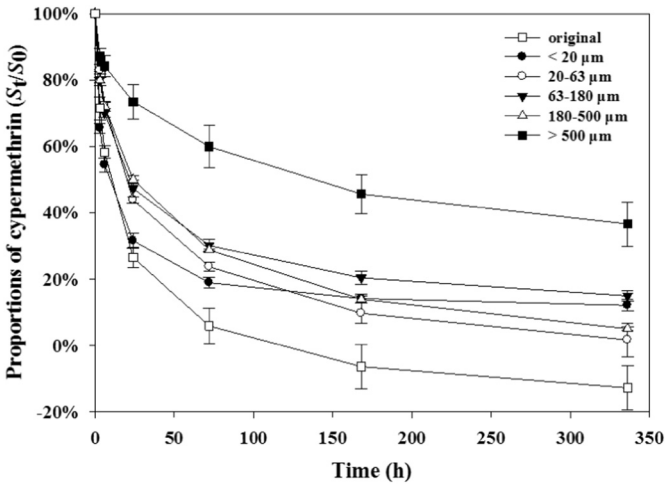

Fig. 2. The desorption curves of cypermethrin in the original and five fractionated sediments determined by consecutive Tenax extraction. Data are shown as the mean ± standard deviation ($n = 3$).

In general, the fine sediment (<20 μm) had higher F_r and k_r values than the coarse sediment (Table 1), indicating larger bioaccessibility and faster desorption of cypermethrin in fine sediments. The $k_{e\text{-SPME}}$ of cypermethrin determined by SPME (or the uptake rate constant of cypermethrin from sediment porewater to SPME fibers) in fine sediments (<180 μm except for 20–63 μm) was slower than that in coarse sediments (>180 μm). Freely dissolved concentration of cypermethrin in sediment porewater determined by SPME (C_{pw}) was generally regarded as bioavailable concentration in sediment. As shown in Table 1, C_{pw} in porewater of fine sediment (<20 μm) was significantly lower than that in other fractions of sediments, suggesting lower bioavailability in fine sediment, which was expected.

The role of sediment particle size in influencing bioaccessibility and chemical activity of cypermethrin was further evaluated by correlating sediment characters (pore volume and TOC) with biomimetic parameters (Figs. S2 and S3, respectively). The F_r increased with increasing pore volume (i.e., decreasing particle size) of the fractionated sediments (Table 1), and the linear regression became significant by excluding the sediment at <20 μm (Fig. S2). The k_r increased with increasing TOC contents by excluding the sediment at >500 μm ($r^2 = 0.90$, $p = 0.052$) due to the much higher TOC content in this sediment (Fig. S3). No significant correlations were observed for the other biomimetic parameters although significant differences of the parameters were noted among the various size fractions (Table 1). Similarly, no significant trends between surface area or quantity adsorbed and the biomimetic parameters were observed. Multiple factors influence sequestration and release of HOCs in sediment (Cornelissen et al., 1999; Kukkonen et al., 2003; Luthy et al., 1997). The surface area, pore volume, and quantity adsorbed are based on physical property, i.e. surface area and porosity of sediments, while the influence of other factors (e.g., the amounts of OC and the quality of organic matter) on the overall adsorption capacity were not included. On the other hand, sediments containing higher TOC contents are expected to exhibit stronger sorption capacity to HOCs. This expected trend was observed for most chemicals in two sediments with different TOC contents, but some exceptions were observed and showed the opposite trend (You et al., 2007), indicating other factors rather than TOC content influenced desorption behavior of HOCs in sediment (Huang et al., 2017). Therefore, it is beneficial to apply a multiple regression to investigate the impact of sediment properties on the adsorption and release of HOCs in sediment, which deserves further study.

As mentioned above, some of the results in the current study were not consistent with previous study, suggesting that other issues rather than particle size were at play. One anomaly encountered was that the original sediment and the smallest size fraction sediment (<20 μm) had higher k_r values than 20–63 and 63–180 μm sediments, however, it was assumed that k_r values would show the opposite trend. During extraction, the extracts of Tenax beads retrieved from the original and

<20 μm sediments showed visual turbidity, indicating fine sediment particles may have been eluted off the beads, while this visual turbidity was not observed in the extracts of beads retrieved from other fractions of sediment. Fine particles are likely to adhere to Tenax beads and/or sorbed by the intraparticle pores of the Tenax beads. Previous studies have shown that Tenax beads have an average intraparticle pore size of about 200 nm and a pore area within each microsphere of approximately 20 nm^2 (Alfeeli et al., 2010; Zhao and Pignatello, 2004). Although the pore size is much smaller than the upper limit of the <20 μm sediment, it is possible that this sediment consisted of particles that were possibly able to fit into this pore size of Tenax beads. The adherence and/or sorption of fine particles by Tenax beads would significantly overestimate the Tenax extractable concentrations, further resulting in overestimation of F_r and k_r (Table 1) in fine sediments and also contribute to the negative desorption curve of the original sediment (Fig. 2). Interestingly, the correlations between sediment pore volume and biomimetic parameters improved for most of the parameters when removing the data of the finest sediment from the analysis (especially for F_r and F_s which had $p < 0.05$) (Fig. S2).

3.3. Bioaccumulation potential of sediment-associated cypermethrin

All water parameters during bioaccumulation test were within acceptable ranges (USEPA, 2000), with dissolved oxygen, temperature, conductivity, pH, and ammonia being 3.4 ± 0.3 mg L^{-1}, 22.6 ± 1.0 °C, 350 ± 7.2 μs cm^{-1}, 7.8 ± 0.2, and 0.3 ± 0.1 mg L^{-1}, respectively. Neither lethal nor sublethal (reproduction and growth) effects were observed for *L. variegatus* during the testing. Lipid contents of the worms exposed to the various fractions of sediment were not significantly different among treatments, as such the mean lipid content (1.12 ± 0.14%) was used for calculation.

The bioaccumulation profile of sediment-associated cypermethrin in *L. variegatus* is shown in Fig. 3. The body residues of cypermethrin reached the highest level at 96 h and started to drop during the remaining exposure period, except for the 63–180 μm sediment which reached its highest concentration at 48 h. Pyrethroids have been reported to be biotransformed in *L. variegatus*, e.g., 37–52% and 57–61% of bifenthrin and permethrin, respectively, were biotransformed in the worms (You et al., 2009). Permethrin was also found to reach the highest concentration in the worms at 96 h and drop during the remaining period in a water-only exposure (You et al., 2009). Induction of enzymes possibly occurred at this time, which significantly increased biotransformation of pyrethroids in the worms and resulted in the drop of body residues of the parent compounds. Due to drop of cypermethrin in the worms after 96 h, the uptake of sediment-associated cypermethrin in the worms were modeled using the first four time points (0, 24, 48, and 96 h). The elimination rate constant of cypermethrin from the worms ($k_{e\text{-}L.v.}$) for the fine sediment (<20 μm) was significantly lower than that for the coarse sediment (180–500 μm) (Table 1). This trend was consistent with the elimination rate constant of cypermethrin from the SPME fiber ($k_{e\text{-}SPME}$), suggesting that SPME fiber acted as an effective surrogate for biota when considering passive partitioning. The large variation of $k_{e\text{-}L.v.}$ for the 63–180 μm sediment (0.059 ± 0.024 h^{-1}) made it difficult to evaluate any trends when including this size.

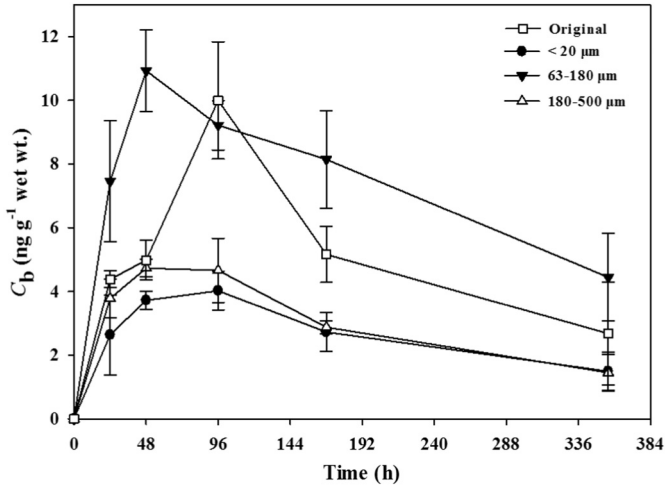

Fig. 3. The time series of cypermethrin concentration in *Lumbriculus variegatus* (C_b) exposed to the original and three different size-distribution sediments.

The BSAF values of cypermethrin in the fractionated sediments ranged from 0.42 ± 0.07 to 0.61 ± 0.04 g OC g^{-1} lipid, which were in the range that was reported in the previous study (You et al., 2009). The BSAF values were lower than 1, supporting the fact that cypermethrin was significantly biotransformed in the worms. The BSAFs of cypermethrin for the three size fractions of sediment (<20, 63–180, and 180–500 μm) were almost the same, suggesting sediment particle size exhibited no significant influence on the bioaccumulation potential of sediment-associated cypermethrin in *L. variegatus*. As discussed above, the elimination (or uptake) rate constant was slower and porewater concentration of cypermethrin was lower in fine sediment than coarse sediment. These two factors (i.e., elimination rate constant and freely dissolved concentration in porewater) are typically used to quantify the uptake of sediment-associated cypermethrin via passive partitioning (Mayer et al., 2014). The difference in these two factors among different size fractions of sediment did not cause the difference in bioaccumulation potential of cypermethrin in *L. variegatus* (expressed as BSAF), suggesting that other exposure routes, e.g., sediment ingestion, may play a role in accumulating cypermethrin by worms from sediments. The contribution of sediment ingestion to accumulating sediment-associated HOCs by benthic invertebrates has been widely recognized, although the quantification through this route requires more investigations (Beckingham and Ghosh, 2017; Sun and Ghosh, 2007; Zhai et al., 2016; Zhai et al., 2018). It has been reported that *L. variegatus* mainly ingest particles smaller than 100 μm, which would significantly impact the actual available pool of sediment-associated HOCs to the organisms (Lawrence et al., 2000; Leppänen and Kukkonen, 2006). Thus, ingesting fine particles would increase the uptake of cypermethrin from the <20 μm sediment by worms, and subsequently increase its body residue which would not be observed in coarse sediment. The results supported the assumption that both desorption and animal behaviors (e.g., feeding behavior) would affect the bioaccumulation potential of sediment-associated HOCs in benthic organisms, although the contribution of particle ingestion to the accumulation of cypermethrin in worms requires further quantification (Wang et al., 2011). The BSAF of cypermethrin in the original sediment was significantly higher than that in the three fractionated sediments (Table 1). As mentioned above, the original sediment consisted mostly of fine particles at <20 μm (81%), implying similar sediment ingestion behavior of worms exposed in these two sediments. Sediment characteristics, including the adsorption capacity and TOC content were similar between these two sediments (Fig. 1). However, the elimination (or uptake) rate constant of cypermethrin by worms in the original sediment was significantly faster than that in the <20 μm sediment, which may result in higher BSAF of cypermethrin in the original sediment.

The rapid desorption concentration ($C_{s\text{-}rap}$) and concentration on SPME fiber at equilibrium (C_f), which were generally regarded as the bioaccessibility and chemical activity, respectively, of cypermethrin in sediment (You et al., 2007), were correlated to the body residues in *L. variegatus* (C_b) at steady state (Fig. S4). The correlations were used to evaluate the effectiveness of Tenax extraction and SPME in predicting the bioaccumulation potential of cypermethrin in different size-distribution sediments. Due to the limited dataset (four size-distribution sediments), the rapid desorption concentrations, concentrations on SPME fiber at equilibrium and concentrations in worms at steady state of HOCs from previous studies were included in the

regression analysis. Significant correlation between C_b and $C_{s\text{-}rap}$ were observed and the datasets of cypermethrin in the different size-distribution sediments (squares in Fig. S4A) were close to the $y = x$ line, suggesting that the rapid desorption concentration determined by Tenax extraction successfully predict the bioaccumulation potential of sediment-associated cypermethrin. In comparison, the regression of the C_b and C_f was under the $y = x$ line, especially for the dataset of cypermethrin in the different size-distribution sediments (squares in Fig. S4B). The C_f was reported to be about 20 times lower than C_b, most likely due to a bias in the equilibrium/steady state in the organisms and SPME fibers (You et al., 2006). In addition, sediment ingestion and biotransformation occur in organisms, but not in the fibers, which may also cause variations between organisms and SPME fibers. However, the consistent trend of elimination (or uptake) rates of cypermethrin from the worms and SPME fibers exposed in different-size sediments (Table 1) suggested that SPME fibers were able to predict the bioavailability of cypermethrin in sediments with different particle sizes.

4. Conclusions

Desorption kinetics, bioavailability, and bioaccumulation potential of cypermethrin in sediments with different particle size distributions were compared in this study. Rapid desorption fractions and rate constants determined by consecutive Tenax extraction significantly decreased with increasing particle size, which were unexpected. Adsorption of fine particles by Tenax beads was one possible reason. Freely dissolved concentration of cypermethrin in porewater of fine sediment determined by SPME was significantly lower than that of coarse sediments, indicating lower bioavailability in fine sediment. The differences in desorption and freely dissolved concentrations of cypermethrin in the size-distribution sediments did not influence the bioaccumulation potential of cypermethrin in the benthic invertebrate *L. variegatus*. Selective ingestion of fine sediment particles by worms may be one reason for the lack of differences. Pyrethroids have been reported to enrich in fine particles in runoff sediments (Gan et al., 2005) and cypermethrin has been identified as a main toxicity contributor to benthic invertebrates in agricultural and urban waterway sediments (Li et al., 2017). Therefore, the differences in kinetics and chemical activity of cypermethrin in sediments with different size distributions observed in the current study may influence their toxicity to sensitive benthic organisms, which deserves further study.

Acknowledgements

This work was supported by the National Natural Science Foundation of China (Grant Number: 41503091 and 41773101), the Natural Science Foundation of Guangdong Province, China (2015A030310219 and 2017A030313065) and the Jinan University (21617452).

Appendix A. Supplementary data

Supplementary data to this article can be found online at https://doi.org/10.1016/j.scitotenv.2018.06.098.

References

Alfeeli, B., Taylor, L.T., Agah, M., 2010. Evaluation of Tenax TA thin films as adsorbent material for micro preconcentration applications. Microchem. J. 95, 259–267.
Beckingham, B., Ghosh, U., 2017. Differential bioavailability of polychlorinated biphenyls associated with environmental particles: microplastic in comparison to wood, coal and biochar. Environ. Pollut. 220, 150–158.
Cornelissen, G., van Zuilen, H., van Noort, P.C.M., 1999. Particle size dependence of slow desorption of in situ PAHs from sediments. Chemosphere 38, 2369–2380.
Di Toro, D.M., Zarba, C.S., Hansen, D.J., Berry, W.J., Swartz, R.C., Cowan, C.E., et al., 1991. Technical basis for establishing sediment quality criteria for nonionic organic chemicals using equilibrium partitioning. Environ. Toxicol. Chem. 10, 1541–1583.
Du, J., Pang, J., You, J., 2013. Bioavailability-based chronic toxicity measurements of permethrin to *Chironomus dilutus*. Environ. Toxicol. Chem. 32, 1403–1411.
Eisma, D., 1993. Suspended Matter in the Aquatic Environment. Springer-Verlag, Berlin, Germany.
Gan, J., Lee, S.J., Liu, W., Haver, D.L., Kabashima, J.N., 2005. Distribution and persistence of pyrethroids in runoff sediments. J. Environ. Qual. 34, 836–841.
Ghosh, U., Gillette, J.S., Luthy, R.G., Zare, R.N., 2000. Microscale location, characterization, and association of polycyclic aromatic hydrocarbons on harbor sediment particles. Environ. Sci. Technol. 34, 1729–1736.
Ghosh, U., Zimmerman, J.R., Luthy, R.G., 2003. PCB and PAH speciation among particle types in contaminated harbor sediments and effects on PAH bioavailability. Environ. Sci. Technol. 37, 2209–2217.
Huang, Y., Zhang, D., Duan, D., Yang, Y., Xiong, Y., Ran, Y., 2017. Importance of the structure and nanoporosity of organic matter on the desorption kinetics of benzo[*a*]pyrene in sediments. Environ. Pollut. 225, 628–636.
Jia, F., Gan, J., 2014. Comparing black carbon types in sequestering polybrominated diphenyl ethers (PBDEs) in sediments. Environ. Pollut. 184, 131–137.
Katagi, T., 2006. Behavior of pesticides in water–sediment systems. Rev. Environ. Contam. Toxicol. 187, 133–251.
Kuivila, K.M., Hladik, M.L., Ingersoll, C.G., Kemble, N.E., Moran, P.W., Calhoun, D.L., et al., 2012. Occurrence and potential sources of pyrethroid insecticides in stream sediments from seven U.S. metropolitan areas. Environ. Sci. Technol. 46, 4297–4303.
Kukkonen, J., Landrum, P.F., 1996. Distribution of organic carbon and organic xenobiotics among different particle-size fractions in sediments. Chemosphere 32, 1063–1076.
Kukkonen, J.V.K., Landrum, P.F., Mitra, S., Gossiaux, D.C., Gunnarsson, J., Weston, D., 2003. Sediment characteristics affecting desorption kinetics of select PAH and PCB congeners for seven laboratory spiked sediments. Environ. Sci. Technol. 37, 4656–4663.
Lao, W., Maruya, K.A., Tsukada, D., 2012. A two-component mass balance model for calibration of solid-phase microextraction fibers for pyrethroids in seawater. Anal. Chem. 84, 9362–9369.
Lawrence, M.A.M., Davies, N.A., Edwards, P.A., Taylor, M.G., Simkiss, K., 2000. Can adsorption isotherms predict sediment bioavailability? Chemosphere 41, 1091–1100.
Leppänen, M.T., Kukkonen, J.V.K., 2006. Evaluating the role of desorption in bioavailability of sediment-associated contaminants using oligochaetes, semipermeable membrane devices and Tenax extraction. Environ. Pollut. 140, 150–163.
Li, H., Cheng, F., Wei, Y., Lydy, M.J., You, J., 2017. Global occurrence of pyrethroid insecticides in sediment and the associated toxicological effects on benthic invertebrates: an overview. J. Hazard. Mater. 324, 258–271.
Luthy, R.G., Aiken, G.R., Brusseau, M.L., Cunningham, S.D., Gschwend, P.M., Pignatello, J.J., et al., 1997. Sequestration of hydrophobic organic contaminants by geosorbents. Environ. Sci. Technol. 31, 3341–3347.
Maund, S.J., Hamer, M.J., Lane, M.C.G., Farrelly, E., Rapley, J.H., Goggin, U.M., et al., 2002. Partitioning, bioavailability, and toxicity of the pyrethroid insecticide cypermethrin in sediments. Environ. Toxicol. Chem. 21, 9–15.
Mayer, P., Parkerton, T.F., Adams, R.G., Cargill, J.G., Gan, J., Gouin, T., et al., 2014. Passive sampling methods for contaminated sediments: scientific rationale supporting use of freely dissolved concentrations. Integr. Environ. Assess. Manag. 10, 197–209.
Mehler, W.T., Li, H., Lydy, M.J., You, J., 2011. Identifying the causes of sediment-associated toxicity in urban waterways of the Pearl River Delta, China. Environ. Sci. Technol. 45, 1812–1819.
Mehler, W.T., You, J., Keough, M.J., Lydy, M.J., Pettigrove, V., 2018. Improvements and cost-effective measures to the automated intermittent water renewal system for toxicity testing with sediments. Ecotoxicol. Environ. Saf. 151, 62–67.
Nutile, S.A., Harwood, A.D., Sinche, F.L., Huff Hartz, K.E., Landrum, P.F., Lydy, M.J., 2017. Methodological and environmental impacts on bioaccessibility estimates provided by single-point tenax extractions. Arch. Environ. Contam. Toxicol. 72, 612–621.
Peng, G., Xiang, N., Lv, S., Zhang, G., 2014. Fractal characterization of soil particle-size distribution under different land-use patterns in the Yellow River Delta wetland in China. J. Soils Sediments 14, 1116–1122.
Qi, Y., Zhang, T., Ren, Y., 2014. Testosterone sorption and desorption: effects of soil particle size. J. Hazard. Mater. 279, 493–501.
Richards, J., Reif, R., Luo, Y., Gan, J., 2016. Distribution of pesticides in dust particles in urban environments. Environ. Pollut. 214, 290–298.
Stehle, S., Schulz, R., 2015a. Agricultural insecticides threaten surface waters at the global scale. PNAS 112, 5750–5755.
Stehle, S., Schulz, R., 2015b. Pesticide authorization in the EU-environment unprotected? Environ. Sci. Pollut. Res. 22, 19632–19647.
Sun, X., Ghosh, U., 2007. PCB bioavailability control in *Lumbriculus variegatus* through different modes of activated carbon addition to sediments. Environ. Sci. Technol. 41, 4774–4780.
Turner, J.S., Pretty, J.L., McDonnell, A.M.P., 2017. Marine particles in the Gulf of Alaska shelf system: spatial patterns and size distributions from in situ optics. Cont. Shelf Res. 145, 13–20.
USEPA, 2000. Methods for Measuring the Toxicity and Bioaccumulation of Sediment Associated Contaminants With Freshwater Invertebrates. EPA/600/R-99/064.
Wang, P., Keller, A.A., 2008. Particle-size dependent sorption and desorption of pesticides within a water-soil-nonionic surfactant system. Environ. Sci. Technol. 42, 3381–3387.
Wang, F., Bu, Q., Xia, X., Shen, M., 2011. Contrasting effects of black carbon amendments on PAH bioaccumulation by *Chironomus plumosus* larvae in two distinct sediments: role of water absorption and particle ingestion. Environ. Pollut. 159, 1905–1913.
Weston, D.P., You, J., Lydy, M.J., 2004. Distribution and toxicity of sediment-associated pesticides in agriculture-dominated water bodies of California's Central Valley. Environ. Sci. Technol. 38, 2752–2759.

Xia, X., Zhang, X., Zhou, D., Bao, Y., Li, H., Zhai, Y., 2016. Importance of suspended sediment (SPS) composition and grain size in the bioavailability of SPS-associated pyrene to *Daphnia magna*. Environ. Pollut. 214, 440–448.

You, J., Landrum, P.F., Lydy, M.J., 2006. Comparison of chemical approaches for assessing bioavailability of sediment-associated contaminants. Environ. Sci. Technol. 40, 6348–6353.

You, J., Pehkonen, S., Landrum, P.F., Lydy, M.J., 2007. Desorption of hydrophobic compounds from laboratory-spiked sediments measured by Tenax absorbent and matrix solid-phase microextraction. Environ. Sci. Technol. (16), 5672–5678.

You, J., Pehkonen, S., Werson, D.P., Lydy, M.J., 2008. Chemical availability and sediment toxicity of pyrethroid insecticides to *Hyalella Azteca*: application to field sediment with unexpctedly low toxicity. Environ. Toxicol. Chem. 27, 2124–2130.

You, J., Brennan, A., Lydy, M.J., 2009. Bioavailability and biotransformation of sediment-associated pyrethroid insecticides in *Lumbriculus variegatus*. Chemosphere 75, 1477–1482.

Zhai, Y., Xia, X., Zhao, X., Dong, H., Zhu, B., Xia, N., et al., 2016. Role of ingestion route in the perfluoroalkyl substance bioaccumulation by *Chironomus plumosus* larvae in sediments amended with carbonaceous materials. J. Hazard. Mater. 302, 404–414.

Zhai, Y., Xia, X., Xiong, X., Xia, L., Guo, X., Gan, J., 2018. Role of fluoranthene and pyrene associated with suspended particles in their bioaccumulation by zebrafish (*Danio rerio*). Ecotoxicol. Environ. Saf. 157, 89–94.

Zhang, B., Li, H., Wei, Y., You, J., 2013. Bioaccumulation kinetics of polybrominated diphenyl ethers and decabromodiphenyl ethane from field-collected sediment in the oligochaete, *Lumbriculus variegatus*. Environ. Toxicol. Chem. 32, 2711–2718.

Zhang, D., Duan, D., Huang, Y., Xiong, Y., Yang, Y., Ran, Y., 2016. Role of structure, accessibility and microporosity on sorption of phenanthrene and nonylphenol by sediments and their fractions. Environ. Pollut. 219, 456–465.

Zhao, D., Pignatello, J.J., 2004. Model-aided characterization of Tenax TA for aromatic compound uptake from water. Environ. Toxicol. Chem. 23, 1592–1599.